DEACTIVATION OF RANEY NICKEL METHANATION CATALYST

ENERGY RESEARCH AND DEVELOPMENT
ADMINISTRATION, PITTSBURGH, PA.
PITTSBURGH ENERGY RESEARCH CENTER
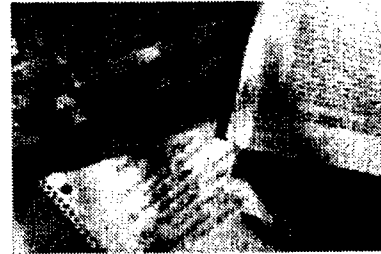
AUG 1977
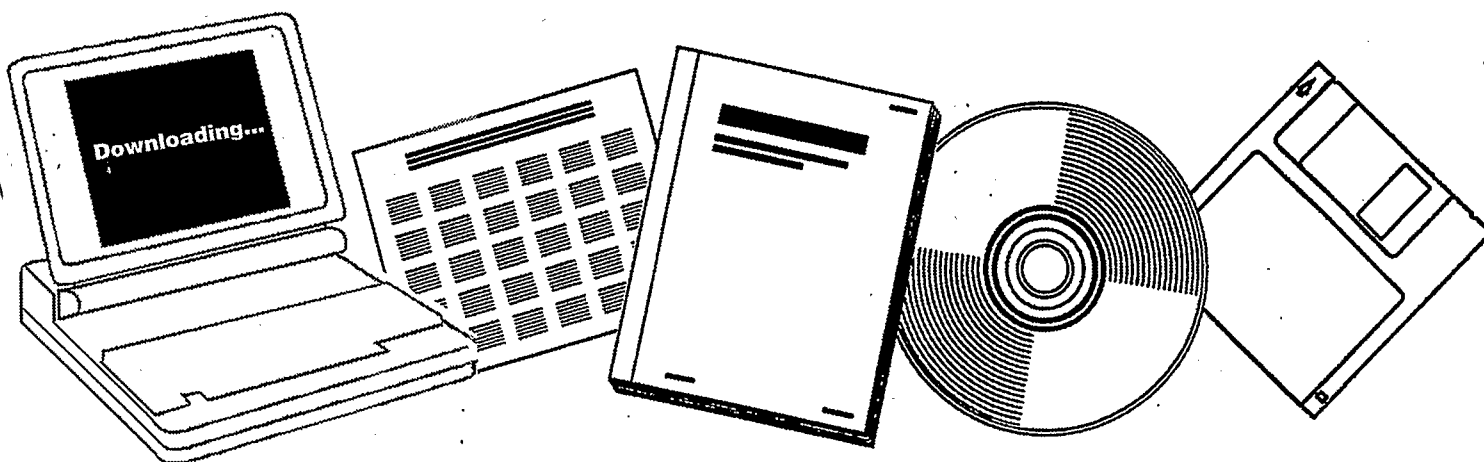
One Source. One Search. One Solution.

NT**i**S

Providing Permanent, Easy Access to U.S. Government Information

National Technical Information Service is the nation's largest repository and disseminator of government-initiated scientific, technical, engineering, and related business information. The NTIS collection includes almost 3,000,000 information products in a variety of formats: electronic download, online access, CD-ROM, magnetic tape, diskette, multimedia, microfiche and paper.
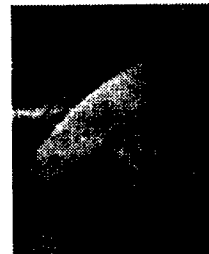
Search the NTIS Database from 1990 forward
NTIS has upgraded its bibliographic database system and has made all entries since 1990 searchable on **www.ntis.gov.** You now have access to information on more than 600,000 government research information products from this web site.

Link to Full Text Documents at Government Web Sites
Because many Government agencies have their most recent reports available on their own web site, we have added links directly to these reports. When available, you will see a link on the right side of the bibliographic screen.

Download Publications (1997 - Present)
NTIS can now provides the full text of reports as downloadable PDF files. This means that when an agency stops maintaining a report on the web, NTIS will offer a downloadable version. There is a nominal fee for each download for most publications.

For more information visit our website:

www.ntis.gov

U.S. DEPARTMENT OF COMMERCE
Technology Administration
National Technical Information Service
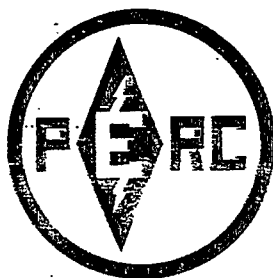Springfield, VA 22161

PERC/RI-77/10
Distribution Category UC-90c

DEACTIVATION OF RANEY NICKEL METHANATION CATALYST

By
R. R. Schehl
H. W. Pennline
A. J. Youngblood
M. J. Baird
J. P. Strakey
W. P. Haynes

Date Published—August 1977

Pittsburgh Energy Research Center
Pittsburgh, Pennsylvania

TECHNICAL INFORMATION CENTER

ENERGY RESEARCH AND DEVELOPMENT ADMINISTRATION

29

TABLE OF CONTENTS

ILLUSTRATIONS

DEACTIVATION OF RANEY NICKEL
METHANATION CATALYST

By

R. R. Schehl, H. W. Pennline, A. J. Youngblood,
M. J. Baird, J. P. Strakey and W. P. Haynes

ABSTRACT

The various mechanisms by which nickel methanation catalysts may
become deactivated are discussed in detail. The analytical data from
spent catalysts removed from pilot-plant-scale reactors are then related
to these deactivation mechanisms. These data represent a number of
lifetime experiments which have been performed over the past six years.

INTRODUCTION

Virtually all of the processes currently under development for the
production of substitute natural gas (SNG) from coal require a catalytic
methanation step for upgrading the raw gas to high Btu pipeline quality.
One of the most promising catalysts for methanation is Raney nickel.
In order for any of the coal-to-SNG processes to become technically
and economically viable, the methanation catalyst should have a life
expectancy of at least one year. Thus far, the maximum life demonstrated
with Raney nickel is about seven months. The objectives of this communication
are to summarize analytical data on spent catalysts from a series of
pilot plant methanation tests, relate the significance of these data to
possible deactivation mechanisms for Raney nickel, and suggest areas for
further concentrated research.

DEACTIVATION MECHANISMS

In general, the models, or intrinsic mechanisms, for catalyst deactivation
may be described by three broad categories. Poisoning or Type I
deactivation, results in a loss of catalyst activity due to the strong
chemisorption of some impurity, generally contained in the feed stream
to the reactor. Type I deactivation is depicted by equation 2.

$$R + s \rightleftharpoons P + s \qquad\qquad (1)$$

$$C + s \rightleftharpoons C \cdot s \qquad\qquad (2)$$

Equation 1 portrays the primary, or desired, reaction. R and P are
the reactants and products, respectively, the the primary reaction and
s represents a catalytically active site. In equation 2, C is considered
to be some contaminant in the feed stream which forms a stable complex
with the site and renders it inactive to the primary reaction.

Type II deactivation encompasses the loss of activity due to reactant
or product degradation of the catalyst surface; coke formation is a
prime example. This model can be further divided into two classifications:

1) the deactivation may be caused by a side reaction involving the same reactants as the primary reaction (parallel fouling); alternately, 2) the deposited or adsorbed material responsible for deactivation may be the result of further reaction of the primary products (series fouling). The parallel and series fouling mechanisms are illustrated by equations 3 and 4, respectively.

$$R + s \underset{\leftarrow}{\rightarrow} R \cdot s \qquad \text{Parallel} \qquad (3)$$

$$P + s \underset{\leftarrow}{\rightarrow} P \cdot s \qquad \text{Series} \qquad (4)$$
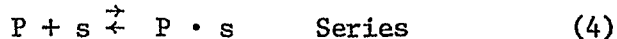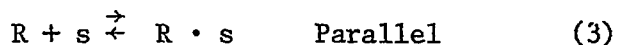
The third category, Type III deactivation, is taken to describe processes which physically alter the catalyst structure, thereby causing a decrease in active metal surface. An example of Type III deactivation is sintering. Sintering is generally thought to be a physical process, akin to thermal annealing, although there exist significant examples of chemically assisted sintering.

There are numerous possible specific mechanisms for the deactivation of Raney nickel when used as a methanation catalyst. The first mechanism, which may be described as Type I, is shown in equation 5.

$$Ni + XH_2S \rightarrow NiS_x + XH_2 \qquad (5)$$
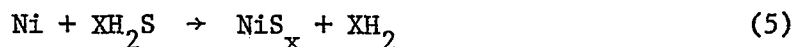
Sulfur rapidly poisons methanation catalysts irreversibly via this reaction. The effect of increasing sulfur concentrations in the feed gas on catalyst life has been clearly demonstrated. In methanation studies at the Pittsburgh Energy Research Center (PERC), effort is made to keep sulfur concentration in the feed gas below 0.1 ppm. Notwithstanding this effort, there exists the possibility of significant cumulative sulfur poisoning in lifetime tests that may last for several thousand hours.

A second Type I mechanism (equation 6) depicts contamination of the Raney nickel surface with iron.

$$Fe(CO)_5 \underset{\leftarrow}{\rightarrow} Fe + 5CO \qquad (6)$$
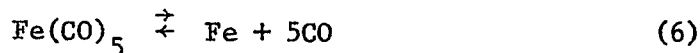
Iron carbonyl can form by reaction of CO at high pressure and low temperature ($100-200°$ C) with carbon steel piping. The carbonyl is carried into the hot reactor where it decomposes according to the reaction shown and deposits on the nickel catalyst. At methanation temperatures, carbon deposition may occur on the iron and further foul the catalyst. Iron concentrations as high as 22 percent have been found in Raney nickel catalyst samples removed from the inlet sections of the reactor. This was also accompanied by high carbon content.

Possible type II deactivation mechanisms for Raney nickel are enumerated below. The first pair of equations describe the deposition of carbon, or coke on the catalyst surface. Equation 7 describes

$$2CO \rightleftharpoons C + CO_2 \quad \text{Parallel} \quad (7)$$

$$CH_4 \rightleftharpoons C + 2H_2 \quad \text{Series} \quad (8)$$
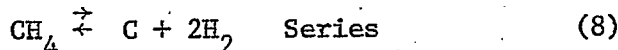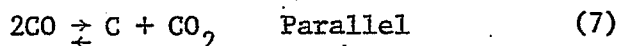
the parallel fouling mechanism of carbon monoxide decomposition while
equation 8 represents the series fouling mechanism of methane decomposition.
Decomposition of carbon monoxide is favored at lower temperatures while
decomposition of methane increases with temperature. As mentioned
above, at methanation temperatures iron promotes this carbon deposition.

Nickel carbide formation as according to equations 9 and 10, is another
possible type II deactivation mechanism. Nickel carbide is found to be

$$XNi + 2CO \rightleftharpoons Ni_XC + CO_2 \quad \text{Parallel} \quad (9)$$

$$XNi + CH_4 \rightleftharpoons Ni_XC + 2H_2 \quad \text{Series} \quad (10)$$
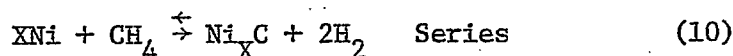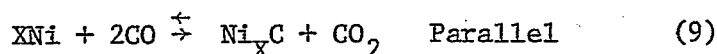
catalytically inactive, but the carbiding can be reversed to reform
an active catalyst by treatment with hydrogen above 250° C. The formation
of Ni_3C can also cause spalling of thermally sprayed Raney nickel catalysts.
Once again, the first equation is the parallel mechanism involving the
reaction of carbon monoxide with nickel to form the carbide while the
second is the series mechanism with methane reacting with nickel to form
nickel carbide. Nickel carbide is generally found in spent samples of
catalyst removed from PERC's methanation reactors. Equation 11 represents
the formation of nickel carbonyl, another possible Type III mechanism.

$$Ni + 4CO \rightleftharpoons Ni(CO)_4 \quad (11)$$
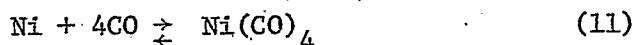
Such a process may cause loss of nickel from the catalyst bed through
vaporization of the formed carbonyl. This forward reaction is not
strictly a Type II mechanism in that the catalyst is not fouled. However,
the reverse reaction may result in the redeposition of nickel on the
catalyst bed in a manner which is not, or at least less, catalytically
active. Whether the nickel is physically removed from the reactor by
the forward reaction, or redeposited by the reverse reaction, both
processes can be most adequately characterized as Type II mechanisms.

Type III deactivation mechanisms are listed in equations 12 and 13. Equation
12 depicts the sintering effect. Nickel crystallites grow in

$$Ni \ (75 \ Å) \rightarrow Ni \ (200 \ Å) \quad (12)$$

$$Ni + [Al] \rightarrow Al + [Ni] \quad (13)$$
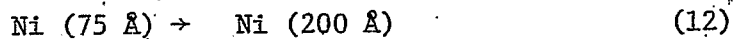
size at an elevated temperature and a loss of surface area results.
Preliminary studies by X-ray diffraction have indicated that the crystallite
size of spent Raney nickel catalyst samples more than doubles in some

instances in comparison to freshly activated catalyst. The second
equation portrays the replacement of surface nickel atoms by aluminum
which was not removed in the activation process. This will be discussed
in more detail later.

REACTOR DESCRIPTION

Basically three different types of pilot-plant-scale methanation reactors,
utilizing thermally sprayed Raney nickel catalyst, have been operated at
PERC throughout the past six years (3, 4, 5, 6, 7, 8, 11, 12). These
reactor systems are: Hot Gas Recycle (HGR) methanator, Tube Wall Reactor
(TWR), and Hybrid reactor (HYB). These reactors have been operated
satisfactorily at space velocities as high as 3000 hr^{-1} and have exhibited
lifetimes as long as four months. Lifetime runs are generally terminated
when carbon monoxide conversion declines to about 95 percent.

The simplest scheme is the Hot Gas Recycle system shown schematically in
Figure 1. Product gas is recycled back to the inlet of the reactor to
dilute the feed and thereby reduce the CO concentration to about 2
percent. Thus, with an inlet gas temperature of about 300° C, the exit
temperature does not exceed 400° C. In the pilot plant a feed gas
containing about 23 percent CO is used with a H_2/CO ratio slightly in
excess of 3/1 for which the required recycle volume is 10 times the feed
volume (10/1). The HGR reactor is illustrated in Figure 2. The primary
advantage of this type of methanator is the low pressure drop through
the bed coupled with its simple design. The low pressure drop is a
result of applying the catalyst to flat plates which are arranged in
parallel and stacked in bundles in the HGR. For these HGR plates Raney
nickel alloy powder (80-200 mesh) is fed through a hydrogen-oxygen flame
where it partially melts and solidifies on the surface of the flat
plate. A bond coat, 0.006" thick, containing 95 percent Ni and 5 percent
Al is first applied to the stainless steel substrate to improve adhesion,
then a coating of Raney nickel, 0.02" thick, is sprayed onto the plate.
Subsequent leaching of the plates with alkali activates the catalyst.
The activated catalyst is kept under hydrogen until contacting with
Syngas at elevated temperature.

Figure 3 illustrates the Tube Wall Reactor System. This is an isothermal
reactor using the heat extraction method to control the heat of reaction.
Although a recycle stream is illustrated in Figure 3, the reactor can
operate with no recycle gas. Raney nickel catalyst is applied to the
inside wall of 2-inch tubes in a heat exchanger bundle. The heat of
the methanation reaction is transferred through the tube wall to boiling
Dowtherm A on the shell side. Reaction catalyst temperature is fairly
high, ca. 390° C, which is about the upper temperature limit of Dowtherm.
A reactor with 7 externally coated 2-inch diameter tubes in a bundle,
27" long, with baffles in the gas space and, more recently, a single
internally coated tube which is 2 inches in diameter by 14 feet long
have been operated. An internally coated TWR is shown in Figure 4.
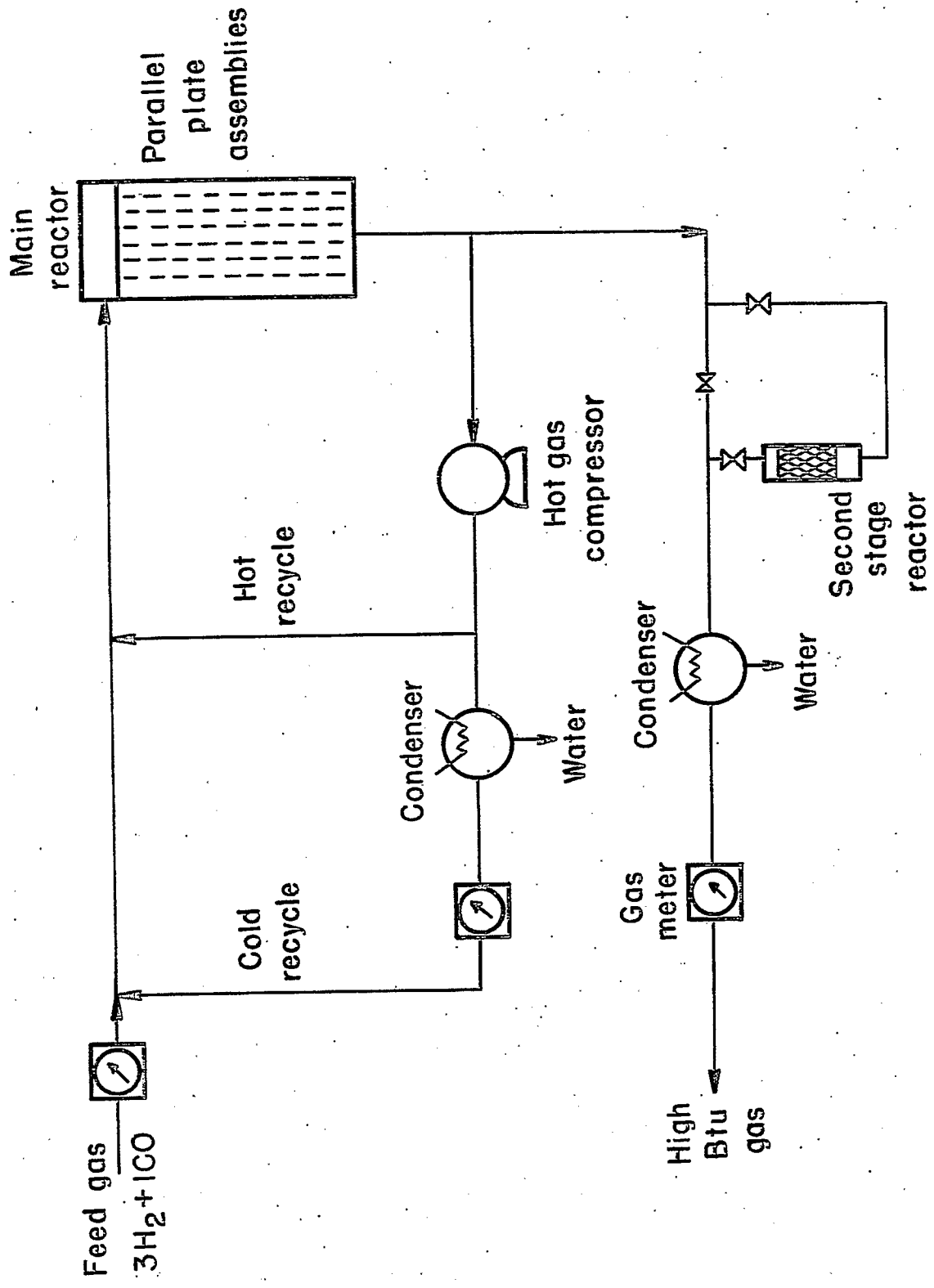
Figure 1. - Flow scheme of the hot-gas-recycle system

Gas inlet

3" pipe sch 40
304 SS

Catalyst grids

Thermocouples
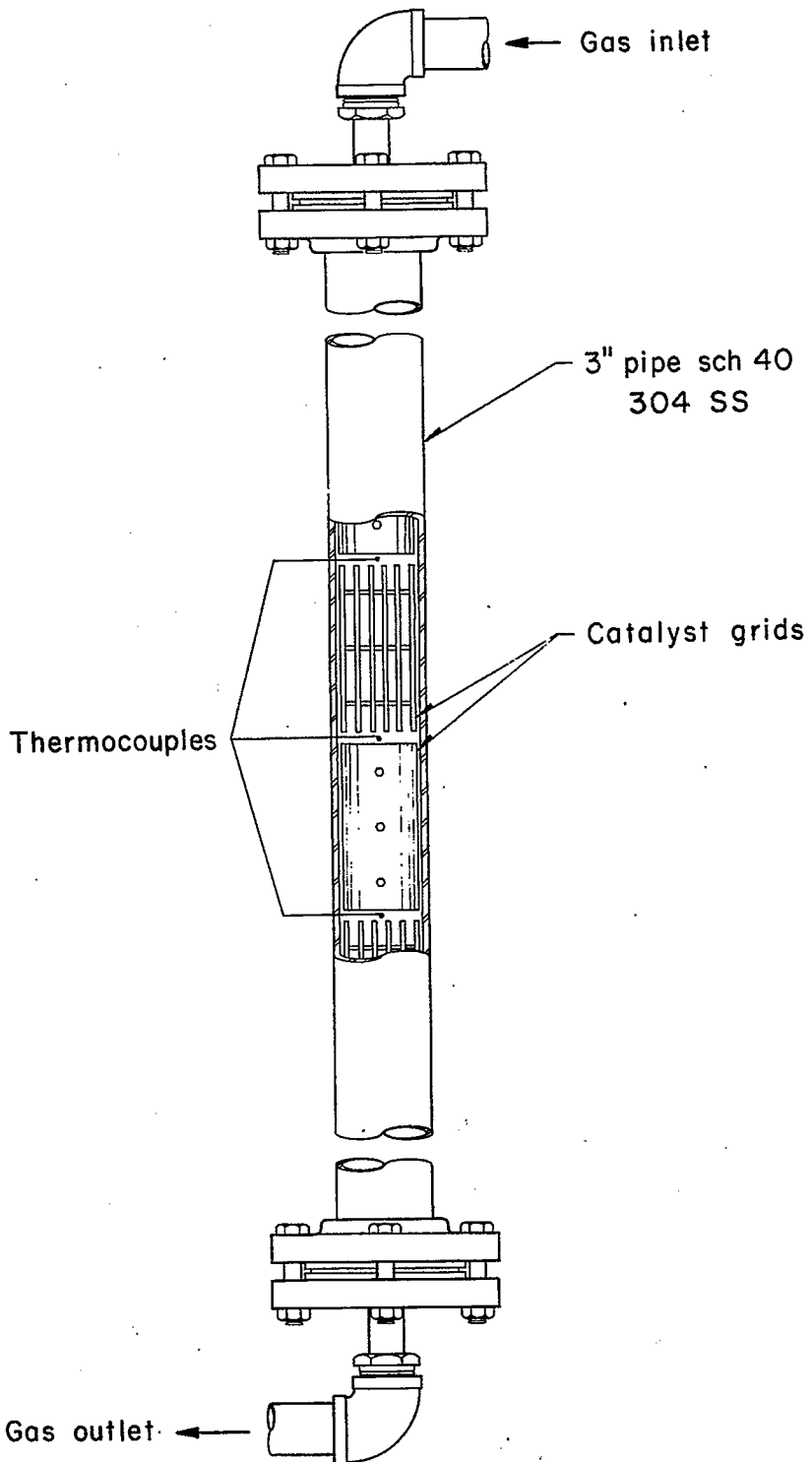
Gas outlet

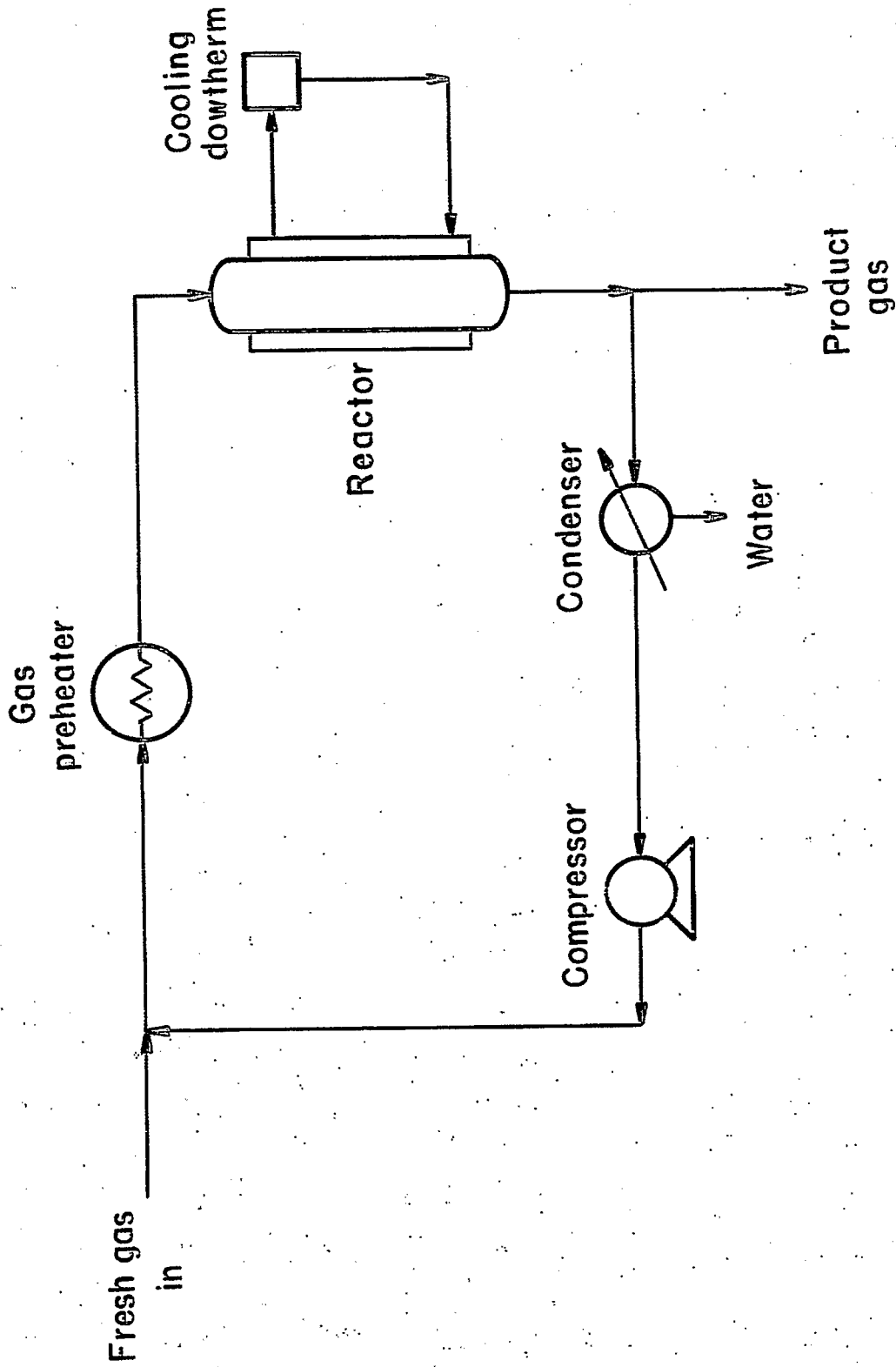Figure 2. - Hot-gas-recycle methanation reactor.

L-13468

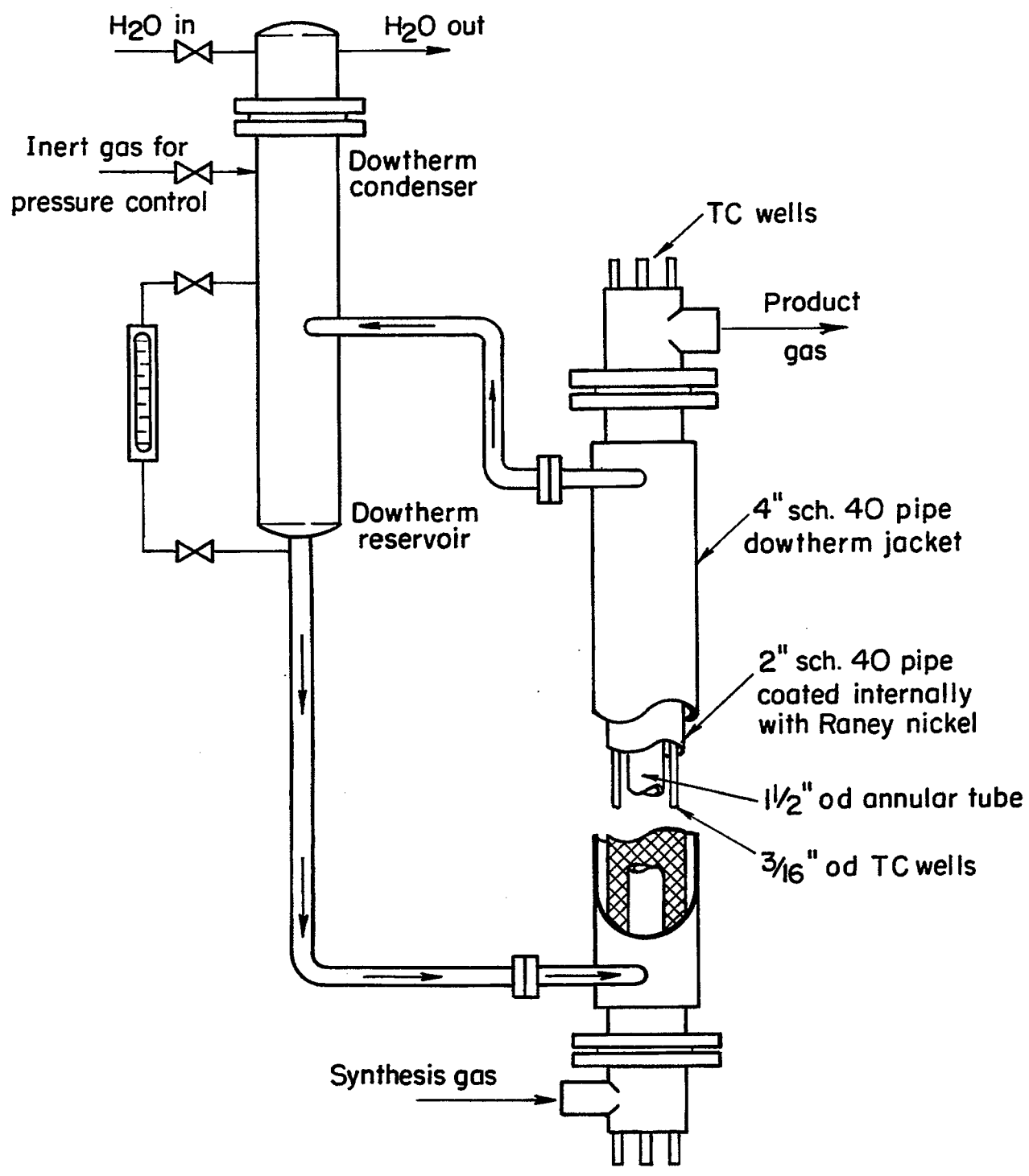Figure 3. - Flow scheme of the tube-wall reactor system.

1-15-76   L-14614

Figure 4. - Tube-wall methanation reactor.

Coating the inside surface of a tube required a specially designed spray
gun and a wire that can be fed down the long barrel. Raney nickel is
brittle and cannot be extruded into a wire form, hence Raney nickel
powder held together in a wire by a plastic binder (20%) is used.
Measured catalyst life has been in excess of 4 months with a high productivity
of 177 mscf CH_4/lb catalyst. The higher operating temperature contributes
to the increased productivity. In smaller bench-scale reactors, catalyst
life has been over 7 months.

A "hybrid reactor" (14) which uses a combination of dilution and heat
extraction for heat removal has recently been developed. X-shaped in-
serts are coated with Raney nickel catalyst and placed in the uncoated
tube wall reactor. This is illustrated in Figure 5. The inlet gas
temperature is 300° C and the Dowtherm temperature is also 300° C.
Recycle is added to control the maximum temperature or "hot spot" at
400° C. With this system, about 65 percent of the heat is removed by
the Dowtherm and the remainder by the sensible heat of the gas.

Recycle can be reduced from the normal 10/1 down to about 6/1. The
principal advantage is that the X-shaped inserts can be easily replaced.
These inserts have a surface area about 15 percent greater than the TWR
and the area can be increased even further by using inserts with more
fins.

Several lifetime experiments have been performed with each of the
reactor systems described above. Table 1 summarizes some of the pertinent
operating conditions and parameters of these experiments.

ANALYSIS OF SPENT CATALYST

Upon termination of a lifetime test, samples of the spent Raney nickel
catalyst are obtained by carefully scraping a portion of the leached
material from the substrate, whether it be an HGR plate, the wall of
the TWR, or the insert used in the Hybrid reactor. Since the catalyst
is exposed to the air at this point, a nickel oxide coating very
likely forms on the surface of any remaining active nickel. These
samples are generally taken from the inlet and exit of the catalyst
bed, and on occasion, from intermediate locations throughout the bed.
The following discussion summarizes the analytical data from the
analysis of these samples.

Initially, the potential Type I deactivation mechanisms will be considered.
Table 2 shows the tabulation of the sulfur concentrations by wet chemical
analysis found in spent catalyst samples. In a few instances (TWR 9,
HGR 12, HGR 14, and HGR 15), there appear to be significant differences
in these bulk sulfur concentrations between the inlet and exit samples.
However, the levels of sulfur are, in general, the same order of magnitude
as that found in unactivated Raney nickel. It must be remembered that
this is a bulk analysis and that a relatively small amount of sulfur on
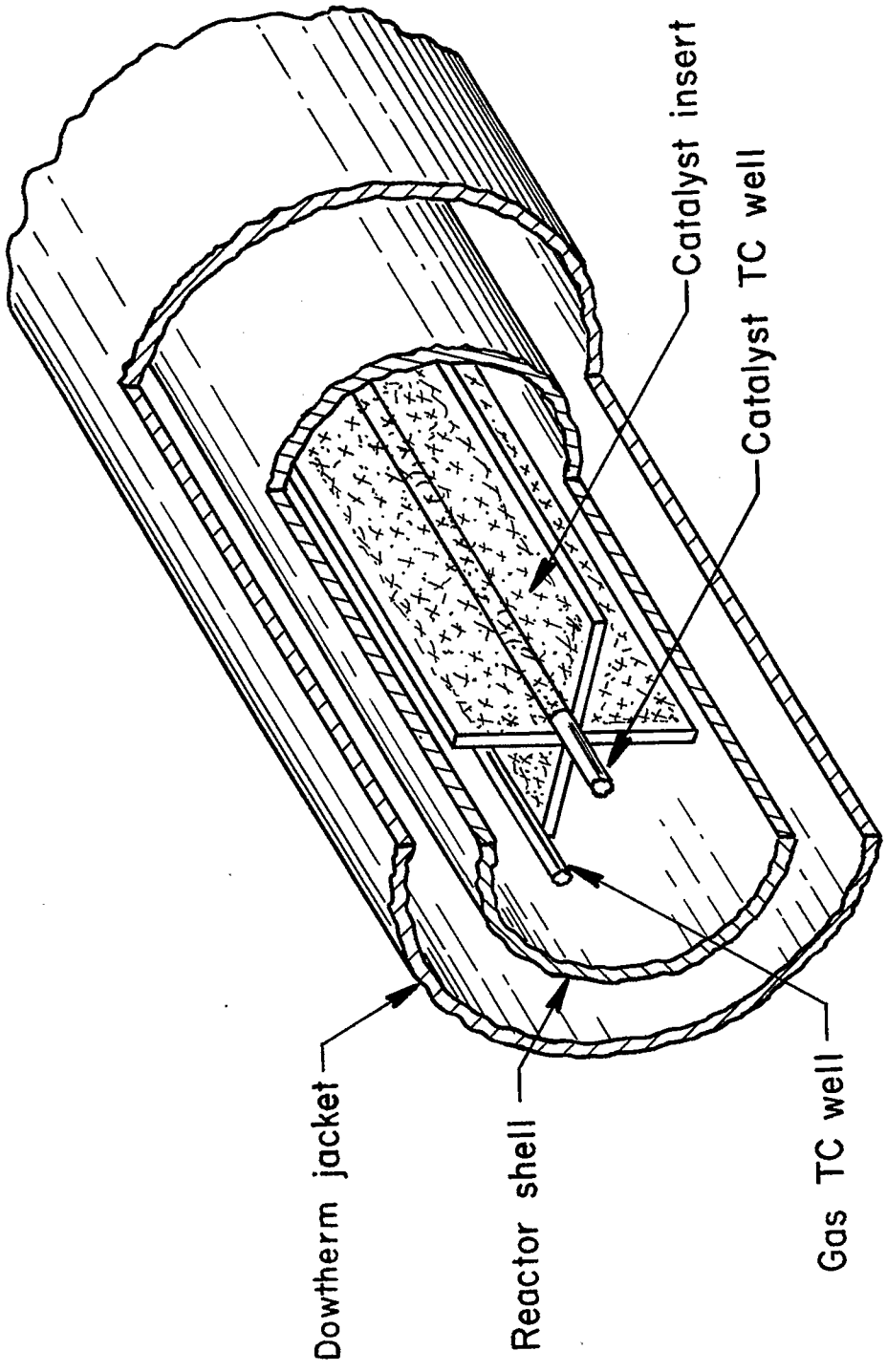
Figure 5. - View of catalyst insert and thermocouple wells.

L-14592

Table 1. - Catalyst Bed Data

Run Number	Catalyst Bed Dimensions	Superficial Catalyst Surface Area, ft^2	Average Exposure Velocity, SCFH/ft2 Catalyst	Length of Test, Hrs.
TWR-6	4" x 8'	8.41	60	2868
TWR-7	Seven 2" externally sprayed tubes, 27" long, enclosed by 8" pipe	8.33	25	1175
TWR-8	4" x 8'	8.41	62	1704
TWR-9	2" x 14'	7.41	60	653
TWR-16	2" x 14'	7.39	25.5	1179
HGR-10	3" x 5'	12.7	16	910
HGR-12	3" x 5'	12.7	26	1400
HGR-14	3" x 2'	11.4	20	2307
HGR-15	3" x 8'	45.64	17	1300
HYB-17	2" x 14'	8.75	31	598
HYB-18	2" x 14'	8.75	39	2073
HYB-19	2" x 14'	7.58	46	1108

[1] Geometric catalyst surface area rather than BET surface area.

the surface of the catalyst might be sufficient to completely, or at least partially, deactivate the catalyst. Indeed, some preliminary investigations of the spent catalyst from two runs, HGR-15 and HYB-18, using surface analysis techniques such as Auger electron and ion scattering spectroscopy (10, 15), have confirmed higher surface concentrations of sulfur at the inlet of the catalyst bed in comparison

Table 2. - Sulfur Concentrations (Wet Chemical Analysis)

	Reactor Inlet	Reactor Exit
TWR 6	0.2%	0.1%
TWR 7	0.2	0.2
TWR 8	0.1	0.1
TWR 9	0.4	0.2
TWR 16	0.2	0.3
HGR 10	0.2	0.2
HGR 12	0.2	0.1
HGR 14	0.2	0.1
HGR 15	0.3	<0.01
HYB 18	0.3	0.3
HYB 19	0.2	0.2

UNACTIVATED RANEY NICKEL: 0.2 -0.3%

to the exit of the bed. Hence, there is direct evidence of some sulfiding of the catalyst surface. Sulfur concentration in the feed stream to the reactor systems, in terms of equivalent H_2S, is normally on the order of 20 ppb. If one assumes that all of the sulfur in the gas stream contacts the catalyst and results in the sulfiding of the nickel surface, a rough calculation indicates that the entire active nickel surface of the bed of a typical hybrid methanator would become sulfided in approximately one year.

The second Type I scheme listed is that of the decomposition of iron carbonyl to leave iron on the nickel catalyst surface. The tabulation of iron concentrations measured at inlet and exit of the catalyst beds is given in Table 3. Iron was measured by atomic absorption which,

Table 3. - Iron Concentrations (Atomic Absorption)

	Reactor Inlet	Reactor Exit
TWR 6	0.2%	0.2%
TWR 7	0.4	0.38
TWR 7	0.4	0.4
TWR 8	0.3	0.3
TWR 9	1.3	1.5
TWR 16	0.5	0.4
HGR 10	22.0	.8
HGR 12	0.4	0.4
HGR 14	1.2	1.2
HGR 15	0.2	0.3
HYB 17	0.3	0.2
HYB 18	0.5	0.7
HYB 19	0.5	0.4

UNACTIVATED RANEY NICKEL: 0.1 - 0.3%

once again, is a bulk analytical technique. In most cases, iron concentrations at the inlet are not appreciably higher than at the exit. The exception is run HGR-10 where 22 percent iron was found at the inlet and only 0.8 percent at the exit. Two catalysts, TWR-9 and HGR-14, had significantly more iron than the others. Again, Auger electron and Mossbauer spectroscopy (11, 16) confirmed higher concentrations of iron in the inlet portions of those samples investigated by these techniques.

Various catalyst samples were analyzed for carbon content as a probe for possible Type II mechanisms. Carbon analysis was performed by the standard ASTM combustion technique and the results are listed in Table 4. It should be noted that, without exception, the concentration

Table 4. - Carbon Concentrations   (Combustion)

	Reactor Inlet	Reactor Exit
TWR 6	5.4%	4.3%
TWR 7	1.5	0.9
TWR 8	2.3	0.25
TWR 9	3.8	1.2
TWR 16	1.3	0.6
HGR 10	13.4	1.9
HGR 12	1.7	0.8
HGR 14	3.5	0.8
HGR 15	4.5	0.9
HYB 17	4.7	0.2
HYB 18	2.0	0.5
HYB 19	3.0	1.1

UNACTIVATED RANEY NICKEL: 0.1 - 0.2%

of carbon is higher at the reactor inlet. In every case but one, the exit of HYB-17, the concentration of carbon is significantly higher than that found in unactivated Raney nickel alloy. Carbon may be present on the catalyst as the result of numerous mechanisms, as previously described: 1) the decomposition of carbon monoxide, 2) the decomposition of methane, or 3) the formation of nickel carbide. The relative importance of these various mechanisms in the carbon deposition problem is unknown at the present time, although decomposition of CH_4 is not likely at the temperatures encountered in the reactors.

Auger electron spectroscopy is capable of distinguishing surface carbidic carbon from amorphous carbon, although this analysis was not performed in the surface studies conducted on these spent Raney nickel catalysts. It was noted in Tables 3 and 4 that inordinately high levels of iron and carbon were found on the catalyst in one particular run, HGR-10. In order to provide more information concerning the shape of the contaminant profiles, spent catalyst was sampled from each of the ten grids used in this experiment. The results are given in Figure 6. Iron and carbon concentration drops sharply after the first two grids and then remains relatively constant at 1-2 percent throughout the rest of the reactor.
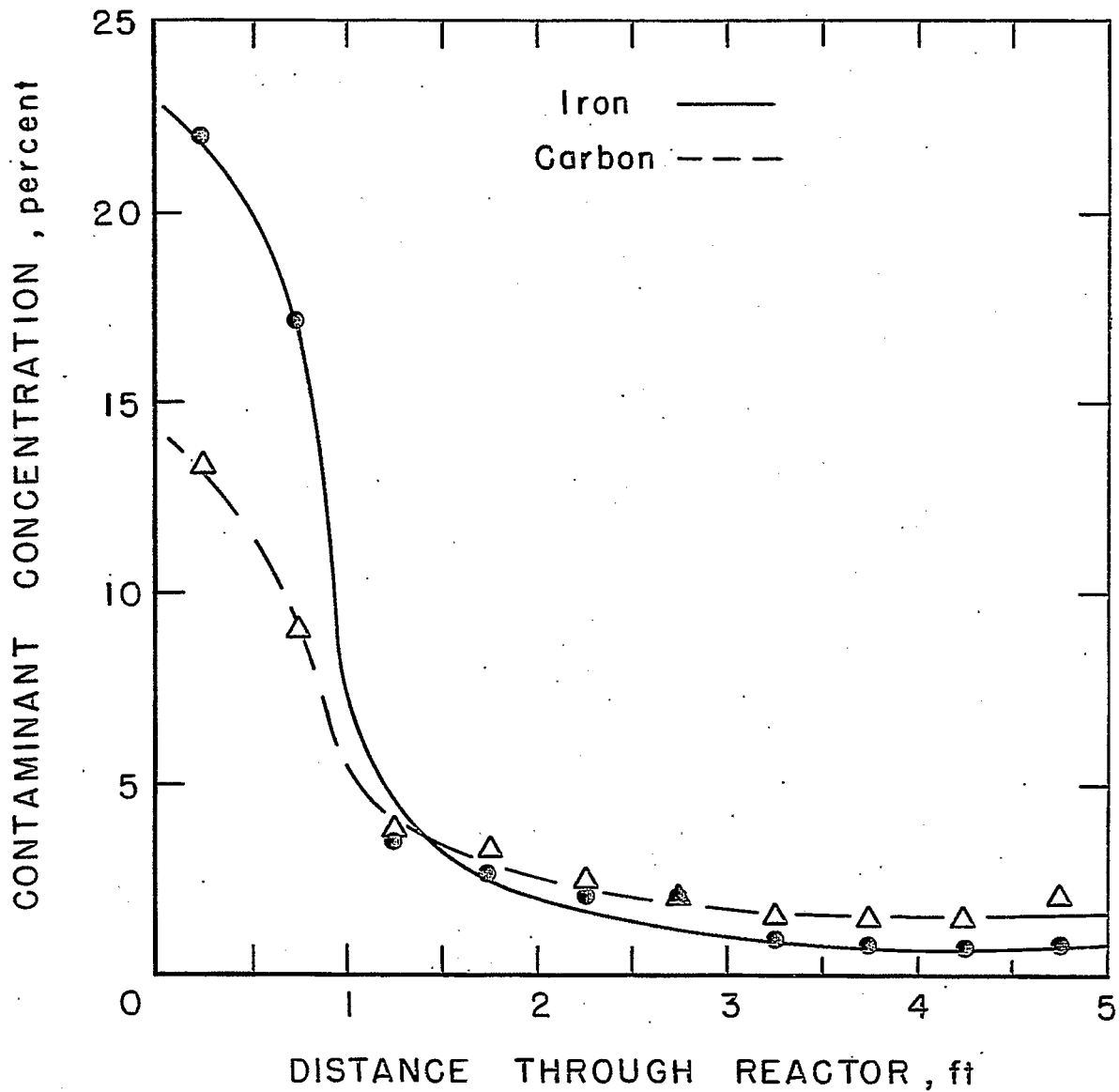
Figure 6. - Iron and carbon concentration profiles from Run HGR-10.

2-26-76   L-14684

The second Type II mechanism discussed was the formation of nickel carbide on the surface of the catalyst. Table 5 illustrates that nickel

Table 5. - Nickel Carbide   (X-Ray Crystallography)

	Reactor Inlet	Reactor Exit
TWR 8	Ni, Ni_3C	Ni
TWR 9	Ni_3C, Ni, $NiAl_3$, Ni_2Al_3, Al	Ni, Ni_3C
TWR 16	$NiAl_3$, Ni_2Al_3, Ni_3C	Ni
HGR 10	Ni_3C, Ni	Ni
HGR 14	Ni, Ni_3C	Ni
HGR 15	Ni, Ni_3C	Ni
HYB 17	Ni_3C	Ni
HYB 18	Ni_3C	Ni
HYB 19	Ni, Ni_3C	Ni
HYB 20	Ni_3C	Ni

carbide is present in all reactor inlet samples. This was the only phase reported for the inlet samples from three of the hybrid reactor tests. Nickel carbide is thought not to be stable above 325° C, although the possibility of the iron contamination somehow stabilizing the nickel carbide has been theorized.

The third Type II mechanism is the removal of nickel from the catalyst bed by formation and vaporization of nickel carbonyl. Nickel carbonyl readily decomposes at our methanation reactor temperatures, although carbonyl detectors at the exit of the methanator have detected carbonyl concentrations as high as 64 ppb.

The first mechanism listed under Type III deactivation is that of sintering. X-ray line broadening measurements indicate that the average

nickel crystallite size for freshly activated catalyst is about 100 Å.
Spent catalyst from the inlet and exit of experiment HGR-15 indicated
crystallite sizes of 175 Å and 225 Å, respectively. This is consistent
with the temperature-time history of the catalyst since the inlet portion
of the catalyst was at 300° C while the exit portion was at 400° C
throughout most of the run.

There exists the possibility of a second type of deactivation arising
from the thermal effects. Surface sensitive techniques such as soft
X-ray appearance potential spectroscopy and Auger electron spectroscopy
have indicated abnormally high surface concentrations of aluminum in
samples of activated Raney nickel catalysts (10). This prompted an
experiment wherein activated Raney nickel was subjected to prolonged
annealing at temperatures in the range of 500 to 600° C. Surface analysis
by soft X-ray appearance potential spectroscopy indicated that the
aluminum concentration on the surface of the catalyst increased as a
result of this heat treatment. It is possible that unleached aluminum
diffuses to the surface at elevated temperatures thus replacing the
original active nickel or that aluminum reaction products from the
activation process migrate from regions below the surface layer as a
result of heat treatment.

MODELING OF THE DEACTIVATION PROCESS

An empirical model for describing the deactivation of thermally sprayed
Raney nickel catalyst beds has been presented (13). The mechanism for
deactivation was assumed to be that of the irreversible adsorption of
compounds, other than the principal reactants or products, on the
catalytically active sites. As defined earlier, this is referred to as
Type I, or independent poisoning. Following the work of Haynes (9), an
irreversible Langmuir-Hinshelwood type of expression was assumed for the
rate of formation of adsorbed poison:

$$r_p = k_p C_p (1 - W/W_s) , \qquad (14)$$

where k_p is the first order rate constant for poisoning, ft/hr, C_p is
the concentration of poison in the stream, lb mol/ft^3, W is the concen-
tration of adsorbed poison on the catalyst surface, lb mol/ft^2, W_s is
the value of W corresponding to complete deactivation of the catalyst,
and r_p is the rate of formation of adsorbed poison, lb mol/ft^2-hr.

In terms of the dimensionless groupings

$$\psi = W/W_s$$

$$\phi = C_p/C_p^o \qquad (15)$$

$$\theta = k_p C_p^o t/W_s ,$$

where C_p^o is the concentration of poison at the reactor inlet, lb mole/ft^3, the equation for the poisoning rate may be expressed as

$$\frac{\partial \psi}{\partial \theta} = \phi \ (1-\psi). \tag{16}$$

Equation 16 can be solved simultaneously with a differential mass balance of the poison species across an element of catalyst surface,

$$\frac{\partial C_p}{\partial a} + \frac{1}{V} \ r_p = 0 \ . \tag{17}$$

The following assumptions must be made if equations 16 and 17 are to describe the temporal and spatial dependence of C_p in the catalyst bed. (1) External mass transfer resistance is neglected; i.e., the poisoning is reaction controlled with the reaction rate given in equation 4. (2) The catalyst is considered to be only an active superficial surface. (3) Volumetric contraction of the gas due to the methanation reaction is neglected.

Substituting equation 14 into equation 17, along with definitions $\lambda = a/a_o$ and $N_p = a_o \ k_p/V$, where a_o is the total superficial catalyst area, we arrive at

$$\frac{\partial \phi}{\partial \lambda} + N_p \ \phi \ (1-\psi) = 0. \tag{18}$$

Equations 16 and 18 must be solved simultaneously for ψ and ϕ as functions of λ and θ. If the catalyst bed is initially free of adsorbed poison and the concentration of poison precursor in the feed remains constant with time, then the following boundary conditions are applicable:

$$\psi(0,\lambda) = 0$$
$$\phi(\theta,0) = 1 \tag{19}$$

The analytical solution of this system is rather tedious. It has, however, been solved in closed form by Bohart and Adams (2) and in more general terms by Amundson.(1) The solution is,

$$\psi(\theta,\lambda) = (1-e^{-\theta})/[1+e^{-\theta}(e^{N_p\lambda}-1)]. \tag{20}$$

The function $\psi(\theta,\lambda)$ may be directly related to the catalyst activity at any point (t,a) as follows

$$A = A_{initial} \ (1 - \psi) \tag{21}$$

provided that the initial catalyst activity is uniform over the entire catalyst bed.

$A_{initial}$ is the preexponential factor in the methanation kinetic rate expression at time zero and A is the local preexponential factor at later times on stream.

The expression for local catalyst activity, equation 21, has essentially three parameters which must be obtained from experimental data: The initial preexponential factor, $A_{initial}$, and two parameters associated with the deactivation process. Transforming equation 20 from dimensionless time and space to real time and space, these two deactivation parameters, p_1 and p_2, are defined as follows:

$$\psi(t,a) = (1 - e^{-p_1 t})/[1 + e^{-p_1 t}(e^{p_2 a}-1)] \qquad (22)$$

Hence, in terms of previously defined quantities, p_1 and p_2 become

$$p_1 = k_p c_p^o/W_s$$

$$p_2 = k_p/V.$$

$A_{initial}$, p_1 and p_2 were evaluated by fitting the model to experimental gas stream temperature profiles measured at five different times during run HGR-15. The average values of the parameters determined by this procedure were then used to predict reactor performance throughout the entire run. Measured and predicted carbon monoxide concentrations in the product gas are compared in Figure 7. Agreement between model and experiment is seen to be remarkably good. The temperature rise across the catalyst bed was increased from 100° to 125° C at 955 hours on stream, thus causing the increased conversion for the last 200 hours.

This same deactivation model, along with the values of the parameters determined for run HGR-15, was used to simulate the catalyst performance in a tube-wall experiment, run TWR-9. This tube-wall reactor was operated with only 3 parts recycled product per 1 part fresh feed and under near-isothermal conditions. Figure 8 illustrates the excellent agreement between experimental values and model predictions. Thus, it is demonstrated that the simple Type I deactivation model outlined above is capable of describing the deactivation of flame sprayed Raney nickel catalyst in two reactors operated under rather dissimilar conditions.

Although the mathematical formulism for this deactivation model is derived from a Type I mechanism, the possibility of some other mode of deactivation being chiefly responsible for the degradation of flame sprayed Raney nickel is not ruled out. For instance, each of the Type II mechanisms which involve carbon monoxide as a reactant (equations 7, 9, and 11) might be expected to develop a deactivation profile similar to that predicted by equation 14. The concentration of carbon monoxide is higher at the inlet portion of the bed, of course, and it is in this region that the catalyst is preferentially deactivated.
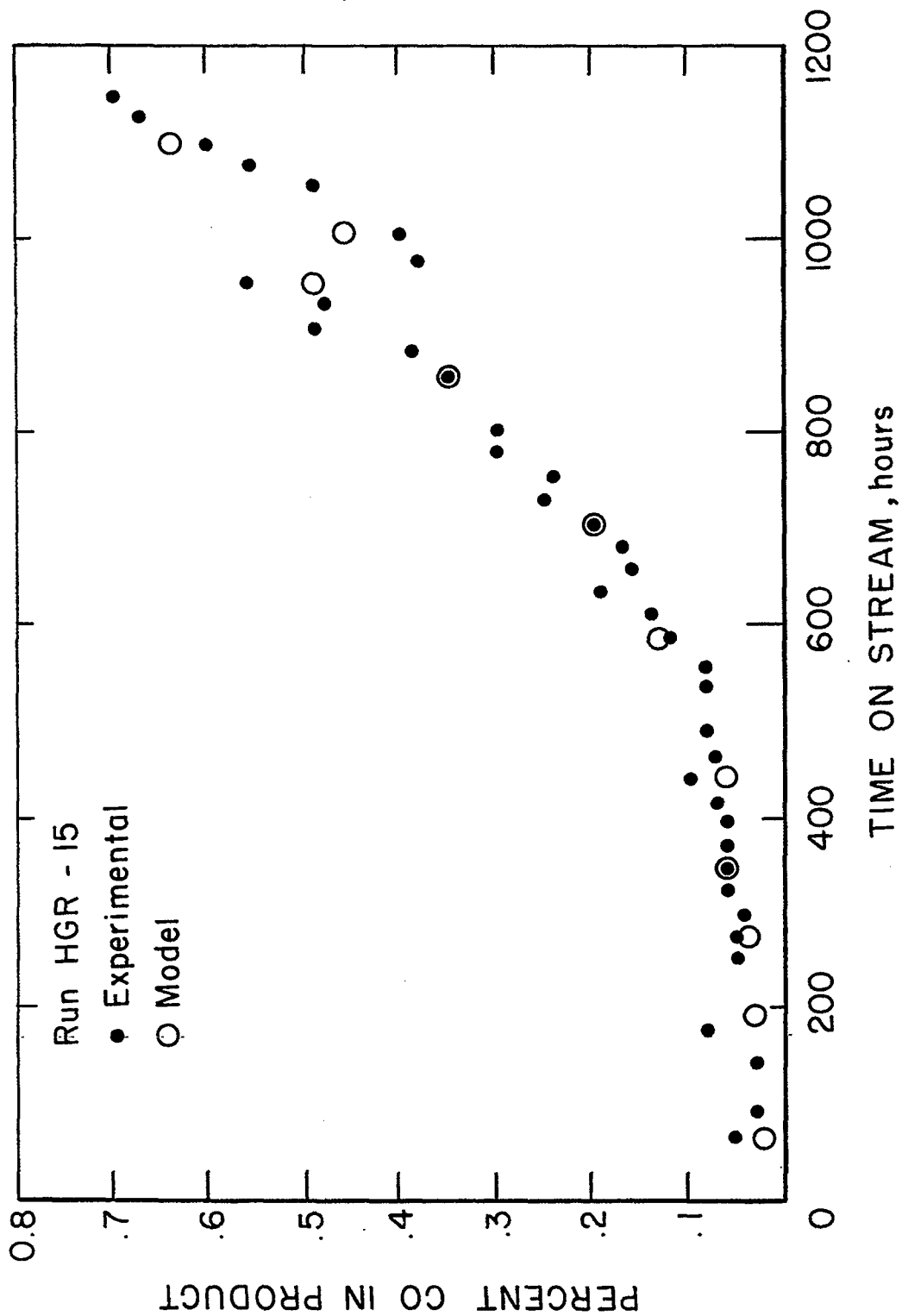
Figure 7. – Carbon monoxide concentrations in the product streams as a function of time of operation from Run HGR-15.
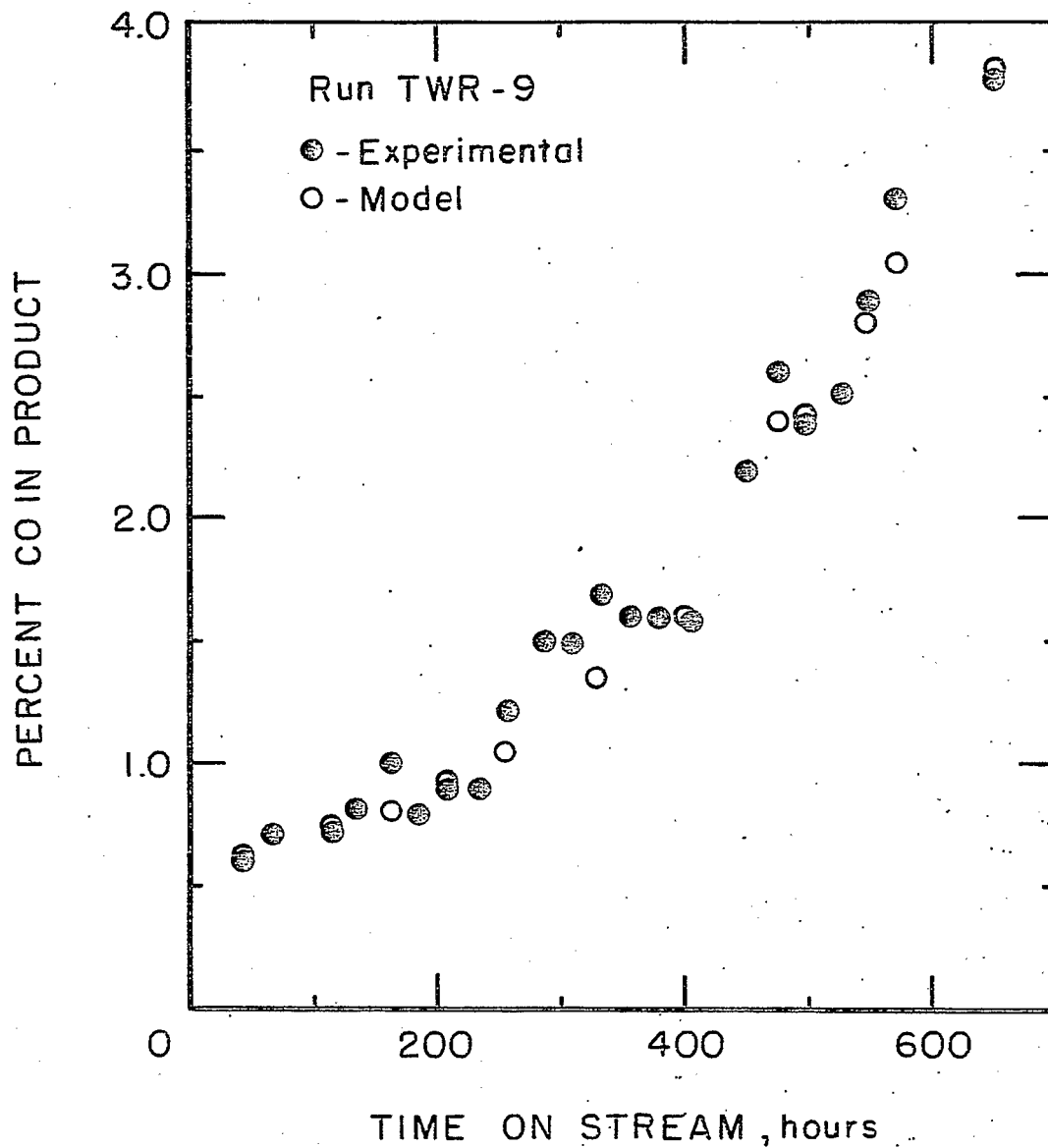
Figure 8. - Carbon monoxide concentrations in the product stream as a function of time of operation from Run TWR-9.

Figure 9 shows a comparison of the calculated relative deactivation profile with measured carbon and sulfur concentrations for run HGR-15. The relative deactivation, $\psi(t,a)$, was calculated for the total time of operation, 1300 hours. Experimentally measured carbon and sulfur concentrations are normalized to unity at the reactor inlet. In effect, by thus normalizing one is assuming that this is the amount of contaminant just sufficient to completely deactivate the catalyst. Figure 9 indicates reasonably good agreement between measured carbon concentrations and the curve predicted by the deactivation model.

SUMMARY

To date, there is no clear evidence that any specific deactivation mechanism is solely responsible for the premature failure of the Raney nickel catalyst used in PERC's pilot plant scale methanation reactors. Indeed, there are experimental data which indicate that each of the seven modes for deactivation is present to some degree. A series of carefully controlled experiments on a smaller scale will be required in order to differentiate the relative significance of each potential contributor to the deactivation process. Several such programs already in progress or in the planning stages at PERC include: 1) iron carbonyl formation, 2) sintering of Raney nickel catalyst, 3) control of carbon formation, 4) significance of sulfur contamination, and 5) catalyst degradation by nickel carbonyl formation-decomposition. It is anticipated that once the prime culprit is identified, provided that there is just one, efforts may be concentrated on the alleviation or control of its effect on catalyst activity.
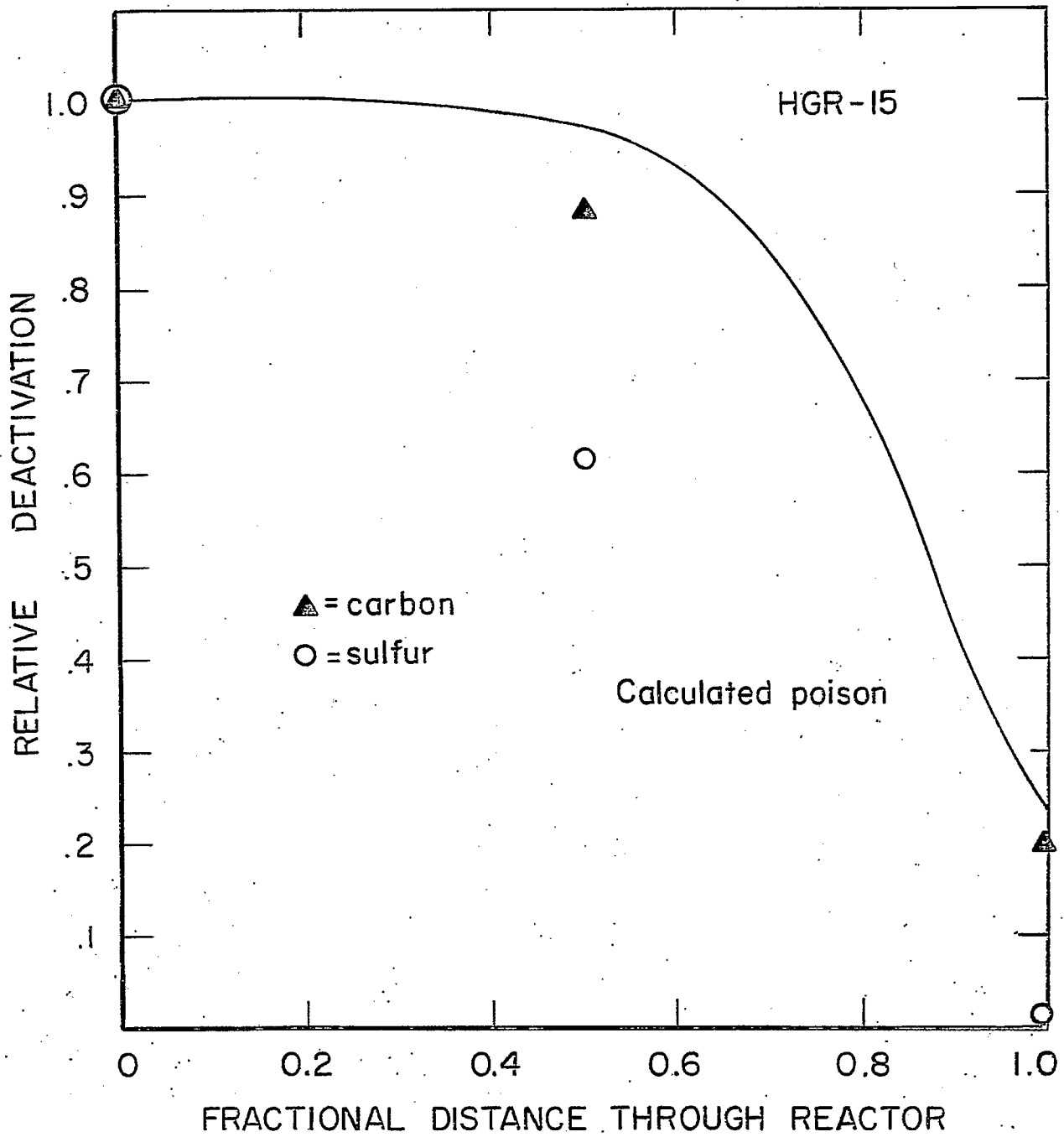
Figure 9. - Poison profiles from Run HGR-15.

REFERENCES

1. Amundson, N. R. A Note on the Mathematics of Adsorption in Beds,
    J. Phys. (Colloid) Chem. 53, pp. 1153-1157, 1948.

2. Bohart, G. S., and E. Q. Adams. Some Aspects of the Behavior of
    Charcoal with Respect to Chlorine, J. Am. Chem. Soc. 42, pp.
    523-544, 1920.

3. Forney, A. J., and J. P. McGee. The SYNTHANE Process - Research
    Results and Prototype Plant Design, Proc. Fourth Synthetic
    Pipeline Gas Symp., Chicago, Illinois, Oct. 30-31, 1972.

4. Forney, A. J., S. J. Gasior, W. P. Haynes, and S. Katell. A Process
    to Make High Btu Gas from Coal, BuMines TPR 24, 1970, 5 pp.

5. Forney, A. J., R. J. Demski, D. Bienstock, and J. H. Field. Recent
    Catalyst Developments in the Hot-Gas-Recycle Process, BuMines
    RI 6609, 1965, 32 pp.

6. Haynes, W. P., R. R. Schehl, J. K, Weber, and A. J. Forney. Pilot
    Plant Study of an Adiabatic Parallel Plate Methanation Reactor.
    Paper presented at the 68th annual meeting of the Am. Institute
    of Chemical Engineers, Los Angeles, Calif., Nov. 16-20, 1975.

7. Haynes, W. P., A. J. Forney, J. J. Elliott, and H. W. Pennline.
    Synthesis of Methane in Hot-Gas-Recycle Reactor Pilot Plant
    Tests, ACS Fuels Division Preprint, Sept. 8-13, 1974, Vol. 19,
    No. 3, pp. 10-42.

8. Haynes, W. P., J. J. Elliott, and A. J. Forney. Experience with
    Methanation in Catalysts, 163d National Meeting of the American
    Chemical Society, Boston, Mass., April 10-14, 1972, Vol. 16,
    No. 2, pp. 47-63.

9. Haynes, H. W. Poisoning in Fixed Bed Reactors, Chem. Eng. Sci.
    25, pp 1615-1619, 1970.

10. Mullendore, A. W., J. E. Houston, M. L. Lieberman, and W. P. Haynes.
    Multi-Parameter Characterization of Deactivation in a Flame-
    Sprayed Raney Nickel Methanation Catalyst presented at the 69th
    Annual AIChE Meeting, Los Angeles, Calif., 1975.

11. Mullendore, A. W., J. E. Houston, M. L. Lieberman and W. P. Haynes.
    A Multi-Parameter Characterization of Deactivation in a Flame-
    Sprayed Raney Nickel Methanation Catalyst. Sandia Laboratories
    Energy Report SAND76-0342, 1976, 32 pp.

12. Ralston, R. D., W. P. Haynes, A. J. Forney, and R. R. Schehl.
    Tube-Wall Methanation Reactors with Combined Diffusion and Kinetic
    Resistance, BuMines RI 7941, 1974, 15 pp.

13. Schehl, R. R., W. P. Haynes, and A. J. Forney. Calculation of
    Catalyst Temperature in a Hot-Gas-Recycle Methanation Reactor,
    ERDA PERC/RI-75/1.

14. Schehl, R. R., W. P. Haynes, and A. J. Forney. Catalyst Deactiva
    tion in Hot-Gas-Recycle Methanation Reactors, A Mathematical
    Model, ERDA PERC/RI-75/3, 1975, 22 pp.

15. Schehl, R. R., H. W. Pennline, J. P. Strakey, and W. P. Haynes.
    Pilot Plant Operation of a Nonadiabatic Methanation Reactor.
    Published in bound volume 21, No. 4 of Preprints of Papers pre-
    sented at 172nd National Meeting of ACS, San Francisco, Calif.,
    Aug. 29-Sept. 3 (1976), pp. 2-21.

16. Yates, J. National Bureau of Standards. Private communication.

Page Intentionally Left Blank

U.S. DEPARTMENT OF COMMERCE
Technology Administration
National Technical Information Service
Springfield, VA 22161   (703) 605-6000